

Experiments on nonlinear wave groups shoaling in a tank

L. Shemer¹, Haiying Jiao² & E. Kit³

Abstract

Evolution of periodically generated wave groups of different shapes that propagate over a sloping beach is studied experimentally and theoretically, by solving numerically the cubic Schrödinger equation. The agreements and disagreements between the experimental and the numerical results are discussed.

Introduction

Real sea waves can be described quite faithfully by JONSWAP spectrum (Hasselmann et al., 1973). One of the important features of this spectrum is its quite narrow frequency band, which results in notable wave groupiness even in the open seas. It has been observed in many field experiments that the distribution of waves in a group approaching the shore becomes more uniform, so that the maximum wave height in the group decreases. Such a transformation of wave groups has important practical consequences, since it affects directly the value of the maximum wave height in the group. The importance of the significant wave height as a design parameter is generally recognized in coastal engineering. This demodulation effect may result from the dissipation in the bottom boundary layer, as well as from the nonlinear and dispersive effects, as shown in numerical simulations based on the Korteweg-de Vries equation by Kit et al. (1995). The reduction in the maximum wave height with decrease of the water depth was also obtained numerically by Barnes and Peregrine (1995). In the present study, the transformation of a deterministic wave group over a sloping beach is investigated experimentally, in a laboratory wave tank, and theoretically, by a numerical solution of

¹ Prof., Dept. of Fluid Mechanics and Heat Transfer, Faculty of Engng., Tel Aviv Univ., Tel Aviv 69978, Israel.

² Ph. D. Student, Dept. of Fluid Mechanics and Heat Transfer, Faculty of Engng., Tel Aviv Univ., Tel Aviv 69978, Israel.

³ Prof., Dept. of Fluid Mechanics and Heat Transfer, Faculty of Engng., Tel Aviv Univ., Tel Aviv 69978, Israel.

model equations. The simplest nonlinear theoretical model which is capable of describing the evolution of propagating wave packet with a narrow spectrum in the range of water depths from deep to intermediate is the so-called cubic Schrödinger equation (CSE) (see, e.g., Mei 1989). This equation was derived first by Zakharov (1968) and Hasimoto & Ono (1972) and has been extensively applied for description of wave group evolution in deep water.

Experimental Facility and Procedure

Experiments are performed in a wave tank that is 18m long, 1.2m wide and filled to a mean water depth of 0.6m. A computer-operated wavemaker is located at one end of the tank. A false bottom made of thick marine plywood is installed in the tank. The effective water depth is 0.3m in the vicinity of the wavemaker. The bottom slope is 1:30 for the length of 7.5m along the tank. The last 5m of the false bottom represent a horizontal flat surface with the effective depth of 0.05m. At the far end of the false bottom is located a wave energy-absorbing beach. Two sets of four wave gauges, each on its own bar, are used in this study. The first set of the gauges is of resistance type, while the second one is of the capacitance type. The distance between the two consecutive probes is 0.4m for the resistance wave gauges and about 0.3m for the capacitance probes. Each probe-supporting bar is mounted on a separate carriage that can be moved along the tank. More sensitive capacitance probes are used for measurements in the shallow water area, while resistance probes are used in the rest of the tank. Detailed measurements of instantaneous surface elevation are carried out at eight fixed measuring stations, thus covering 32 locations along the tank.

Wave groups with three different shapes are selected in this study. The equations describing the driving signal applied to the wavemaker are as following:

$$s(t) = A_0 \sin(\Omega t) \sin(\omega t), \quad \Omega = \omega / 20 \quad (1)$$

$$s(t) = A_0 |\sin(\Omega t)| \sin(\omega t), \quad \Omega = \omega / 20 \quad (2)$$

$$s(t) = A_0 \exp - (t / 5T)^2 \sin(\omega t), \quad (3)$$

$$-16T < t < 16T$$

where the carrier wave period $T = 2\pi/\omega$. These signals are repeated periodically. The first two driving signals produce identical wave groups envelopes, but their spectra differ essentially. The forcing signal (1) has a simple bimodal spectrum. The spectrum of (2) consists of a set of discrete frequencies, where 3 dominant modes can be identified. The third signal produces wave groups that are widely separated and have a discrete spectrum, which requires a considerable number of modes for its accurate description. Experiments are carried out for $T=0.7$ s and for three values of the driving amplitude A_0 , corresponding to a nearly linear, nonlinear, and strongly nonlinear wave steepnesses. In the vicinity of the wavemaker, the maximum values of the wave steepness $\alpha_0 k_0$ in the group are approximately 0.07, 0.14 and 0.21. Variation of the wave group velocity along the tank and modification of the wave power spectra are measured.

Theoretical Model

The cubic Schrödinger equation (CSE) for a mild slope is selected as the theoretical model. The CSE is written in a form given by Mei (1989):

$$-i\mu A - iA_X + \alpha A_{\tau\tau} + \beta |A|^2 A = 0 \tag{4}$$

where $A(X, \tau)$ is the complex wave group envelope, and the slow variables are related to the coordinate along the tank x and the time t as

$$X = \epsilon^2 x; \quad \tau = \frac{1}{\epsilon} \int \frac{dX}{c_g(X)} - \epsilon t \tag{5}$$

In (5), $c_g = \partial\omega/\partial k$ is the group velocity, k being the local wave number, and $A(X=0, \tau=0) = a_0/\epsilon$. The local values of the X -dependent coefficients in the CSE are defined in the dimensionless form by

$$\frac{\mu}{k_o} = \frac{dq}{dX} \frac{(1 - \tanh^2 q)(1 - q \tanh q)}{k_o [\tanh q + q(\tanh^2 q)]}, \tag{6}$$

$$\frac{\alpha\omega^2}{k_o} = \frac{\omega^2}{k_o c_g^3} \frac{\partial^2 \omega}{\partial k^2}, \tag{7}$$

$$\frac{\beta}{k_o^3} = \frac{1}{n} \left[\frac{\cosh 4q + 8 - 2 \tanh^2 q}{16 \sinh^4 q} - \frac{1}{2 \sinh^2 2q} - \frac{(2 \cosh^2 q + n)^2}{\frac{q}{\tanh q} n^2} \right], \tag{8}$$

where $q = kh$, $k_o = k(X=0)$ and the parameter $n = c_g k/\omega$ represents the local value of the ratio of group and phase velocities and is given by

$$n = \frac{1}{2} \left(1 + \frac{2q}{\sinh 2q} \right). \tag{9}$$

It is well know that the coefficient β of the nonlinear term given by (8) and (9) changes its sign at $q=1.36$. For $q>1.36$, $\beta>0$, corresponding to the focusing condition, while for $q<1.36$, $\beta<0$ and wave energy defocusing occurs. The radian frequency of the carrier wave ω is related to its wave number k by the dispersion relation

$$\omega^2 = kg \tanh q, \tag{10}$$

where g is the acceleration due to gravity. Equation (4) is solved numerically using an implicit finite difference scheme with periodic in τ boundary conditions. Initial conditions at $X = 0$ are in accordance with the shapes defined by (1) to (3). The variation of the surface elevation η is obtained using the complex amplitude $A(X, \tau)$ from the solution of (4) and the relations (5) between the scaled (X, τ) and the physical (x, t) variables as

$$\eta(x, t) = \varepsilon [A(X, \tau) e^{i(kx - \omega t)} + c.c.], \tag{11}$$

where *c.c.* denotes complex conjugate.

Results and Discussion

The results for the wave groups excited by the driving signal given by the equations (1) – (3) are presented in Figures 1 – 3, respectively, for the two extreme values of the forcing amplitude, $a_0 k_0 = 0.07$ and $a_0 k_0 = 0.21$.

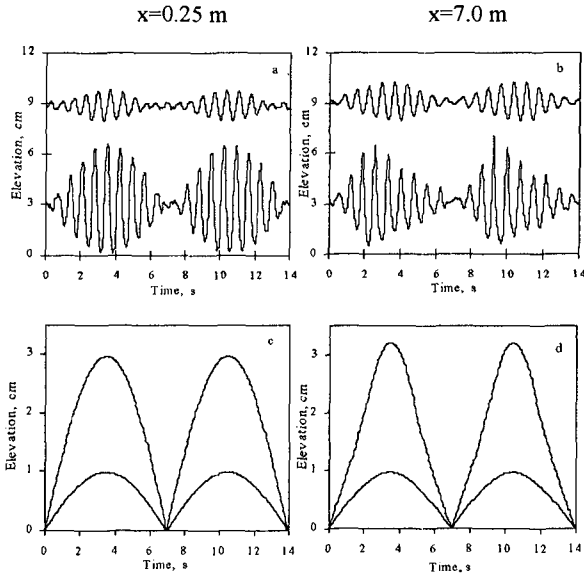


Figure 1. The measured surface elevation (*a* and *b*) and the computed group envelopes (*c* and *d*) for the driving signal (1).

In each Figure, the results are given at two locations along the tank, $x = 0.25$ m, $h = 0.3$ m (Figures *a* and *c*), and $x = 7.0$ m, $h = 0.075$ m (Figures *b* and *d*). The measured variation in time of the instantaneous surface elevation is given in Figures *a* and *b*, where the curves representing the low and the high amplitudes are shifted in the vertical

direction. The corresponding variation in time of group envelopes obtained numerically is given in Figures *c* and *d*.

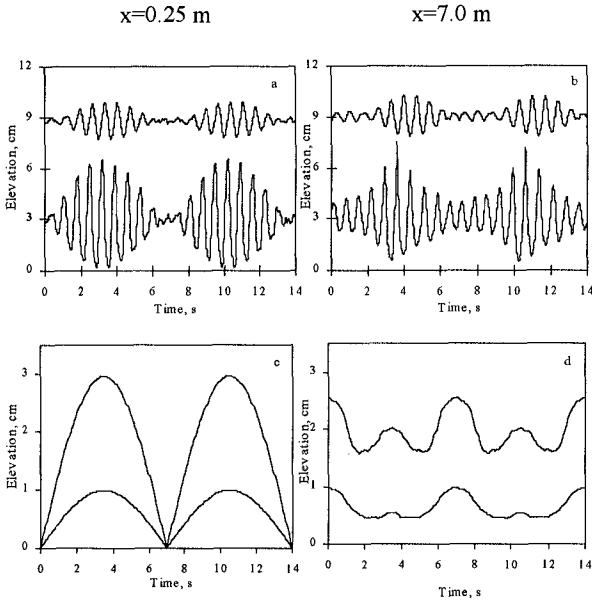


Figure 2. The measured surface elevation (*a* and *b*) and the computed group envelopes (*c* and *d*) for the driving signal (2).

The most striking effect observed in this study is the difference in the evolution of wave groups excited by the driving signals (1) and (2). In the vicinity of the wavemaker, both types of wave groups look practically identical, see Figures 1*a* and 2*a*. At a larger distance, the wave groups generated by (1), Figure 1*b*, tend to retain their identity, although nonlinear effects are clearly visible, while the wave groups excited by (2), Figure 2*b*, are spread significantly. This spreading can be interpreted as the demodulation effect. Certain spreading can also be observed in the detached wave groups excited using (3), Figure 3*b*. For all shapes of the forcing signals, the initially symmetric wave groups at higher amplitude lose their symmetry. The trough-crest asymmetry is clearly visible at high amplitude of forcing at both locations. This asymmetry is a clear indication of the appearance of the higher harmonics in the surface elevation spectrum. In addition to the trough-crest asymmetry, left-right asymmetry is observed at the remote measuring station at high amplitude of forcing. This effect is most prominent for the driving signal (3), Figure 3*b*, although it also can be observed in Figure 1*b*. Note that similar group shapes were observed in experiments and obtained numerically in deep water by solving the modified nonlinear Schrödinger equation (Lo & Mei 1985).

The demodulation effect observed in the experiments away from the wavemaker is clearly seen in the numerical simulation as well, Figure 2*d*. Contrary to that, wave group shapes for the forcing signals (1) and (3) do not change notably, although certain focusing effects can be observed at high amplitude of forcing in Figures 1*d* and 3*d*. It should be mentioned here that the left-right asymmetry observed in the experiments could not be obtained in the framework of the adopted theoretical model, since the CSE conserves the symmetry of the initial conditions. In Figures *c* and *d*, the envelope corresponding to the temporal variation of wave groups at the carrier frequency only is presented, and the contribution of the bound waves at higher harmonics, which leads to the trough – crest asymmetry observed in the experiments, is not accounted for.

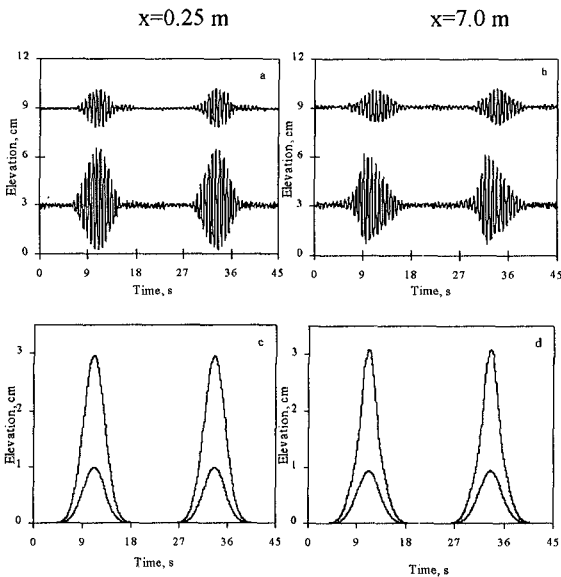


Figure 3. The measured surface elevation (*a* and *b*) and the computed group envelopes (*c* and *d*) for the driving signal (3).

Both the experimental and the numerical results indicate that for the driving signals (1) and (3) no considerable variation in the maximum wave amplitude can be observed for the conditions employed in this study. For the driving signal given by (2), both the experiments and the computations give considerable spreading of the wave energy in the group. The results presented in Figures 1 – 3 thus suggest that the adopted theoretical model is capable of providing a reasonable pattern of wave group evolution over a sloping beach. The CSE can therefore be used to investigate the wave group evolution over larger distances, which could not be verified experimentally due to the limitations of the experimental facility.

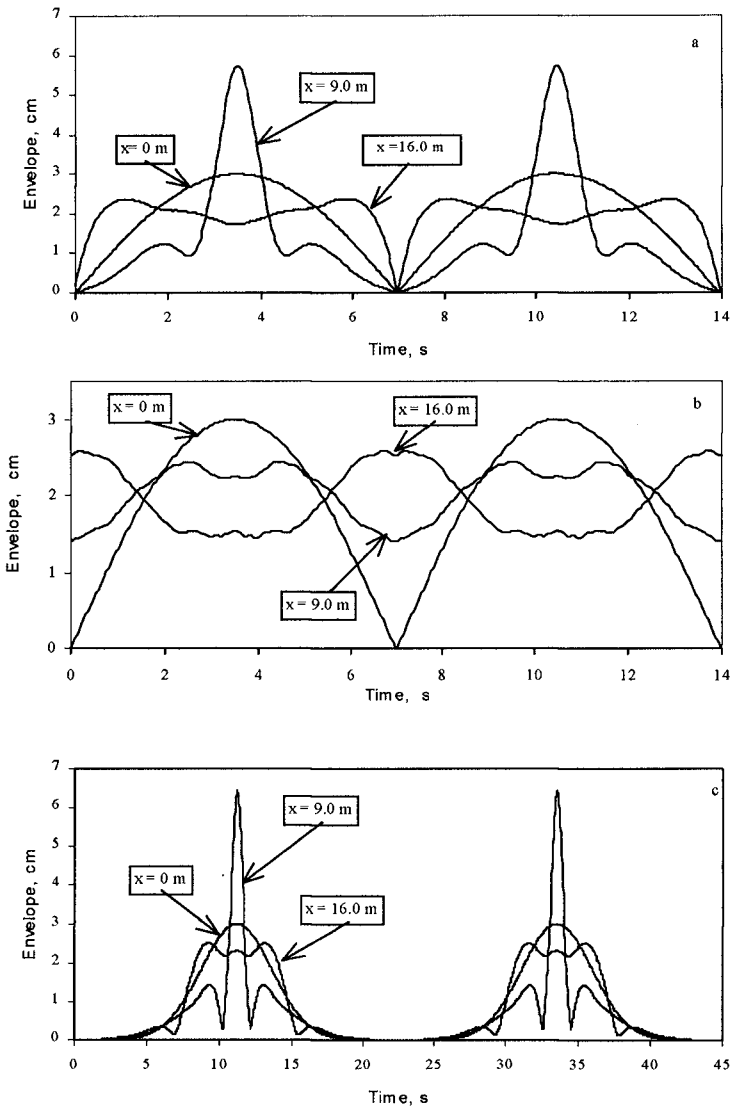


Figure 4. The computed variation of the wave group envelopes with the distance from the wavemaker for the bottom slope 1:30; initial depth $h=0.6$ m. *a)* driving signal (1), *b)* driving signal (2), *c)* driving signal (3).

Computations were therefore performed wave groups of high wave steepness ($a_0k_0 = 0.21$) for the driving signals given by (1) to (3) for the same slope of 1:30 as in the experiments, but with the initial depth of $h=0.6$ m. The results at three locations along the tank for the duration corresponding to two wave groups are presented in Figure 4. The locations selected for the presentation correspond to the initial wave group at the wavemaker, $x=0$ m, $h=0.6$ m, intermediate depth at $x=9.0$ m, $h=0.3$ m, and shallow water at $x=16.0$ m, $h=0.067$ m.

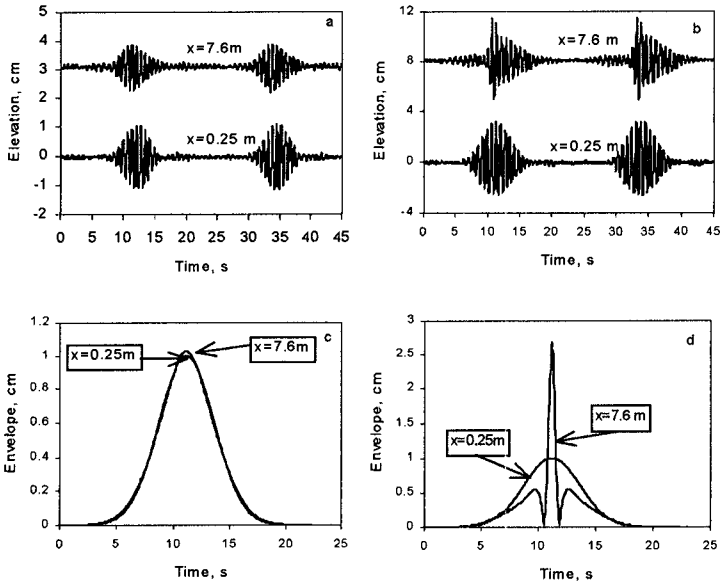


Figure 5. The measured surface elevation (*a* and *b*) and the computed group envelopes (*c* and *d*) for the constant water depth $h=0.6$ m and the driving signal (3).

The qualitative difference in the evolution pattern of wave groups excited by signal (1), Figure 4*a*, and (2), Figure 4*b*, is quite evident. The wave groups excited by the driving signal (1) initially exhibit strong focusing, and the maximum amplitude is nearly doubled at $x=9.0$ m. As the waves propagate over more shallow water, strong defocusing occurs, and the wave energy is spread nearly uniformly in the group. It should be stressed here that due to the symmetry properties of the driving signal (1) and the CSE (4), the node points in the envelope distribution in time are conserved in the course of the evolution process. This particular feature does not apply to the driving signals (2) and (3). The qualitative difference between the driving signals (1) and (2) is responsible for the different evolution patterns on Figures 4*a* and 4*b*. Contrary to Figure 4*a*, no strong

focusing is observed at the initial stages of evolution for the driving signal (2), and at both locations in Figure 4b, $x=9.0$ m, $h=0.3$ m, and $x=16.0$ m, $h=0.067$ m, the waves are distributed essentially uniformly along the group.

Evolution pattern for the detached groups in Figure 4c is similar qualitatively to that observed in Figure 4a. Here too, the wave energy is initially focused at $x=9.0$ m, $h=0.3$ m. At larger distances from the wavemaker and in more shallow water demodulation is obtained. Although the driving signal (3) does not require conservation of the node points as it is the case for the signal (1), the groups are initially sufficiently separated, so that no substantial interference between the neighboring groups can occur for the time and length scales employed in the present computations.

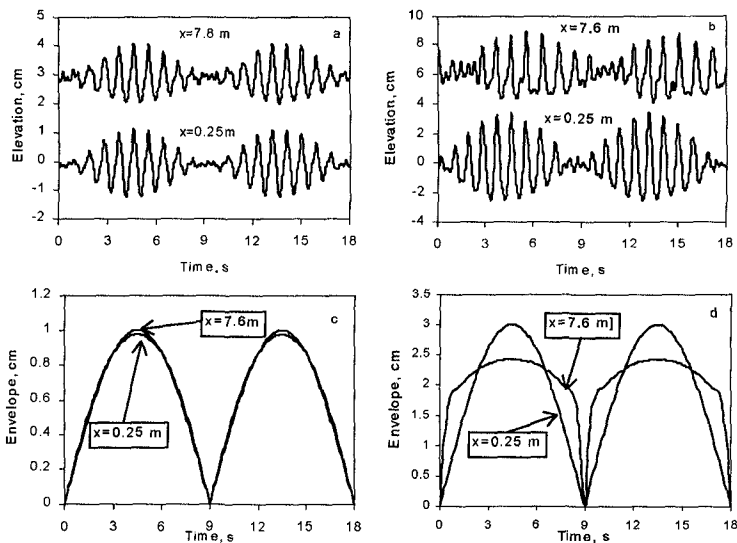


Figure 6. The measured surface elevation (*a* and *b*) and the computed group envelopes (*c* and *d*) for the constant water depth $h=0.6$ m, $T=0.9$ s and the driving signal (3).

These computational results suggest that it may be instructive to study wave group evolution in water of constant depth. The representative experimental and numerical results for the two extreme forcing amplitudes ($a_0 k_0 = 0.07$ and $a_0 k_0 = 0.21$) for the deep ($h=0.6$ m) and shallow ($h=0.012$ m) water cases are given in Figures 5 and 6, respectively. The driving signal (3) is used in the results of Figure 5, while the signal (1) is employed in Figure 6.

For the conditions of Figure 5, focusing (increase in the maximum wave amplitude within the group) is obtained for the high forcing amplitude both in the experiments

(Figure 5*b*) and in computations (Figure 5*d*). For the low amplitude of forcing, no significant variation of the maximum wave amplitude along the tank is obtained in Figures 5*a* and 5*c*.

In shallow water the spreading of the wave energy is obtained experimentally for the high amplitude of forcing in Figure 6*b*. The corresponding demodulation effect is observed in the numerical simulations presented in Figure 6*d*. At low amplitude of forcing, no significant effects are observed neither in experiments (Figure 6*a*), nor in computations (Figure 6*c*).

A more detailed analysis of the evolution of nonlinear wave groups in water of a constant intermediate depth is presented in Shemer et al. (1998). The experimental results are compared in this study with the numerical solutions of the CSE. In an additional study, Kit et al. (1998), nonlinear wave group evolution in shallow water is investigated. The measurements of the temporal and spatial variation of the instantaneous surface elevation are supported by the numerical solutions of the Korteweg-de Vries equation.

Concluding remarks

The present study indeed confirms that wave groups propagating over a sloping beach undergo modulation and subsequent demodulation and their wave energy tends eventually to spread more uniformly over the group. In the case of the constant water depth, defocusing is obtained in shallow water, while in deeper water, the trend is opposite and wave energy focusing leading to increase of the maximum wave height above its initial value is observed.

The current investigation reveals that shoaling wave groups having identical initial envelope shapes but different spectral contents may undergo completely different evolution processes. Specifically, groups having a bimodal spectrum, driving signal (1), retain their clear identity in the process of propagation, and their envelope periodically attains zero. For wave groups with the same shape and more complicated spectra, driving signal (2), the wave energy tends to become more uniformly distributed along the group, so that the clear distinction between the groups vanishes.

The simplest possible nonlinear model, the cubic Schrödinger equation, which contains an additional term accounting for mild water depth variation and is thus capable of describing wave group shoaling, is selected here. The coefficient of the nonlinear term in this equation changes its sign in the course of wave group propagation toward the beach.

The total body of experimental and numerical results accumulated in this study indicates that the cubic Schrödinger equation (4) constitutes a reasonable model for studies of shoaling of nonlinear gravity wave groups over a sloping beach. CSE appears to be able to capture successfully the global features of nonlinear wave group transformation for the whole range of the water depth variation employed here. It also reflects correctly

in general the effect of the initial maximum wave steepness $k_0 a_0$ on the group evolution pattern. The CSE thus can be considered as a robust, albeit crude model for description of the nonlinear wave group evolution and transformation in water of slowly varying depth.

Acknowledgement

This work was supported in part by a grant from the Israel Science Foundation.

References

Barnes, T., and Peregrine, D.H. 1995 Wave groups approaching a beach: full irrotational flow computations. Int. Conf. on Coastal Research in Terms of Large Scale Experiments, Abstracts, Poland, 7 - 8.

Hasimoto, H. and Ono, J. 1972. "Nonlinear modulation of gravity waves." *J. Phys. Soc. Japan* 33, 805-811.

Hasselmann, K., Barnett, T.P, Bouws, E., Carlson, H., Cartwright, D.E., Enke, K., Ewing, J.A., Gienapp, H., Hasselmann, D.E., Krusemann, P., Meerburg, A., Müller, P., Olbers, D.J., Richter, K., Sell, W., and Walden, H. 1973 "Measurements of wind-wave growth and swell decay during the Joint North Sea Wave Project (JONSWAP)." *Deut. Hydrogr. Z.*, 8, (suppl. A).

Kit, E., Pelinovsky, E. and Talipova, T. 1995 Transformation of probability distribution of wind waves in coastal zone. Proceedings of the COPEDEC IV, Brazil, v. 3, 2344-2353.

Kit, E., Shemer, L., Pelinovsky, E., Talipova, T., Eitan, O., and Jiao, H. 1998 Nonlinear wave group evolution in shallow water. Submitted for publication.

Lo, E. and Mei, C.C. 1985 A numerical study of water-wave modulation based on a higher-order nonlinear Schrödinger equation. *JFM* 150, 395-416.

Mei, C.C. 1989 "The Applied Dynamics of Ocean Surface Waves." World Scientific, Singapore.

Shemer, L., Kit, E., Haiying Jiao, and Eitan, O. 1998 Experiments on nonlinear wave groups in intermediate water depth. *J. Waterway, Port, Coastal and Ocean Engng.*, v. 124. Zakharov, V.E. (1968). "Stability of periodic waves of finite amplitude on the surface of deep fluid." *J. Appl. Mech. Tech. Phys.* 2, 190-194.

Zakharov, V.E. 1968 "Stability of periodic waves of finite amplitude on the surface of deep fluid." *J. Appl. Mech. Tech. Phys.* 2, 190-194.